© پیش‌نویس مجله علمی محاسبات نرم، برای داوری در مجله

An Intelligent Model to Diagnose the Brain Connections Disorders in ADHD People in Different Frequency Bands

Elham Askari [1*], Assistant professor

[1] Department of Computer Engineering, Fouman and Shaft Branch, Islamic Azad University, Fouman, Iran.
Elham.Askari@iau.ac.ir

Abstract: Attention deficit hyperactivity disorder is a neurodevelopmental disorder that typically begins in early childhood and poses significant challenges during school years. This disorder is characterized by impulsive behaviors, inattention, and difficulties with concentration. Early diagnosis and prompt treatment can effectively manage this condition. Accurate diagnosis of ADHD can be achieved through the precise analysis of electroencephalography signals. This article proposes a brain modeling approach using a cellular neural network in various frequency bands to diagnose ADHD. Firstly, the inter-area connections in the brains of individuals with hyperactivity are estimated by assessing the spectral coherence function between channels. Subsequently, the intra-area connections are obtained using a cellular neural network. The results obtained indicate that the intra and inter-area connections in the central, frontal, and parietal regions of the brains of individuals with hyperactivity differ from those of normal individuals in the beta and gamma frequency bands. Consequently, it can be inferred that the presence of disparities in intra and inter-area connections between the brains of individuals with ADHD and normal individuals results in distinct brain functionality within these two groups.

Keywords: *Brain; Attention Deficit Hyperactivity Disorder; Electroencephalography; Cellular Neural Network; Spectrogram*

SCJ Accepted

*** Corresponding author**

1. Introduction

Attention deficit hyperactivity disorder (ADHD) is a condition characterized by difficulties in paying and maintaining attention mentally. The symptoms of this disorder in adults can manifest in various ways, including changeable relationships, bad jobs or academic performances. While ADHD typically emerges in childhood, there are cases where it may not be diagnosed until adulthood. Psychologists diagnose this disorder based on the American standard diagnostic criteria (DSM-IV-TR)[1].

Hyperactivity is typically categorized into three types, each of which is briefly discussed below. The first type is attention deficit disorder, characterized by a person's difficulty in concentrating and being easily distracted. The second type is hyperactivity disorder, in which individuals are excessively physically active, constantly jumping and running. They struggle to remain seated and tend to be overly talkative. The third type is combined disorder, which encompasses both hyperactivity disorder and attention deficit disorder [2].

Electroencephalography has been instrumental in diagnosing and studying hyperactivity disorder in individuals [3]. Given the intricate nature of the information derived from EEG signals, it is crucial to employ appropriate features for analysis. By accurately recording these electrical signals and subjecting them to meticulous processing, it becomes feasible to extract valuable information and features. Through comparative analysis and study of these processed signals, it is possible to diagnose various brain and mental disorders with a high degree of accuracy.

In recent years, numerous researchers have focused on leveraging machine learning and signal processing techniques to identify and diagnose diverse mental and brain disorders by extracting crucial features from these signals. Various machine learning methods have been employed to achieve this goal. These methods involve the utilization of expert knowledge and skills to implement algorithms, incorporating the significant features extracted from the data [4, 5].

Muller et al. introduced a machine learning system that employed support vector machine (SVM) classification to distinguish hyperactive adults from healthy control groups. Their approach relied on measuring the characteristics of event-related potentials derived from EEG signals for the classification process [6, 7].

In the study conducted by Chandana et al., various brain regions were examined in individuals with hyperactivity. The research aimed to investigate potential differences between the brain areas of hyperactive individuals and healthy individuals in two states: eyes closed and eyes open. The researchers employed neural networks and extracted energy characteristics within the alpha, beta, gamma, and theta frequency bands to distinguish between the two groups [8].

Moriguchi and Hiraki employed near-infrared spectroscopy to measure proxy features related to brain function in individuals with hyperactivity [9]. They highlighted the utility of near-infrared spectroscopy in measuring cerebral blood flow, which provides valuable insights into brain activity [10].

SVM is a method that has shown promise in improving accuracy in detecting hyperactivity [11]. Yasumura et al. utilized SVM to analyze brain activity and diagnose hyperactivity specifically in the frontal region of the brain. Their study reported an overall accuracy rate of 86.26% in identifying hyperactivity [12].

Metsis et al. developed a novel sparsity-based feature selection method for identifying array comparative genomic hybridization (aCGH) data that can aid in classifying different disease subtypes. This method effectively reduces the number of features by employing a regression model or SVM to shrink irrelevant coefficients, resulting in the elimination of those features [13, 14].

SCI Accepted

Mohammadi et al. proposed an approach to distinguish children with ADHD from healthy children using EEG signals recorded during a specific task. They extracted nonlinear features such as fractal dimensions, approximate entropy, and Lyapunov view from the EEG signals for diagnosis. By applying the mRMR (Minimal Redundancy Maximal Relevance) method and DISR (Double Input Symmetrical Relevance) method using a multilayer perceptron (MLP), they achieved accuracies of 92.28% and 93.65%, respectively [15].

Mogadam et al. utilized EEG fractality extraction for diagnosing ADHD. They employed the graph coloring algorithm to analyze connectivity networks, representing functionally connected brain areas, along with EEG fractality. Their findings demonstrated a deficit in communication between the occipital and frontal lobes in ADHDs [16].

In another study, He et al. employed a convolutional neural network-LSTM model to process EEG data for high-accuracy classification. They observed that ADHD patients exhibited predominantly short range connections, whereas the normal group displayed long-range connections between the occipital lobe and left anterior temporal areas [17].

Motamed et al., in a 2022 study, distinguished between healthy individuals and those with hyperactivity using FFT features and PCA feature reduction. They employed a convolutional neural network model to separate the two groups and achieved an accuracy of 91% [18].

Taghibeyglou et al. conducted a study using electroencephalography (EEG) to diagnose ADHD. They achieved 95.8% accuracy in identifying this disorder by employing convolutional neural network and classical machine learning models [19].

Loh et al. employed ECG data and a 1D convolutional neural network to classify ADHD and normal groups. They utilized the gradient-weighted class activation mapping function to highlight crucial ECG features at specific time points that significantly impacted the classification score. Their approach yielded a diagnostic accuracy of 96.4% for ADHD [20].

Bakhtiari et al. introduced a new feature extraction method using the evaluation of dynamic connectivity tensors among EEG electrodes for building the input formula of the classification model. These tensors encompass correlations between EEG channels in various time intervals, allowing for the preservation of spatial and temporal structures of the EEG data while reducing input dimensions of the model. They utilized a convolutional short-term memory network to differentiate between ADHD and normal children [21].

One of the biggest challenges in the diagnosis of ADHD is the lack of attention and insufficient attention of computer engineering and medical engineering researchers to this issue. Most of the studies that have been done so far have examined the connections of brain areas and how their parts work without using a single model. After examining the electroencephalographic signals of ADHD people, this article will find a model using cellular machine learning for the brain pattern of hyperactive and normal children. In addition, the way of organizing and connecting the areas of the two groups and their differences are shown. In this article, with the help of features extracted from EEG signals and neural networks, the brain pattern of hyperactive and healthy people will be obtained. The presented model is able to present the general and partial function of the brain and has the ability to present the differences in the brain connections of people with hyperactivity.

This article is organized in such a way that after the introduction, the proposed method is presented in the second part. In the third part, the results will be analyzed and in the fourth part, the conclusion will be expressed.

2. Materials and Method

SCI Accepted

The proposed model is designed based on brain architecture and function and includes three main phases: In the first phase, pre-processing and preparation should be done on the signals. The 3 minutes noise-free parts are selected for each person, and then normalization and filtering are done. In the second phase, the design of the proposed model is done, and in the third phase, the obtained results will be analyzed. The proposed method is shown in figure (1), diagramatically. In the following, all the steps will be explained in detail.

2.1. Database

The database used includes EEG signals with the protocol of character recognition in the cartoon and counting the number of characters. The number of 121 signals was recorded, of which 61 people were diagnosed with ADHD and 60 of them were diagnosed as normal. 10-20 standard with 21 scalp electrodes and 128 Hz sampling rate was used for recording. Electrodes include Fp1, Fp2, F3, F4, F7, F8, Fz, Cz, Pz, C3, T3, C4, T4, P3, P4, T5, T6, O1 and O2 and reference electrodes A1 and A2. The age range of people with ADHD is 7 to 12 years. The database is accessible from the site (https://ieee-dataport.org/open-access/eeg-data-adhd-control-children). The 3 minutes noise-free parts are selected for each person and this 3 minutes is divided into 5 second parts (640 epochs).

2.2. Wavelet Transform

The electroencephalography signal is decomposed into different bands using the wavelet transform. In this article, the signal is decomposed into alpha, beta and gamma bands. By filtering the signal with high-pass filter H(n) and low-pass filter L(n), the frequency domain is cut and decomposed into A and D coefficients. This approximation operation produces a set of approximate coefficients. Equation (1) calculates the wavelet transform of the continuous signal x(t) in the function ψ, with the scale a and the transfer parameter b [22, 23].

$$CWT(a,b) = \int_{+\infty}^{-\infty} x(t)\frac{1}{\sqrt{|a|}}\Psi(\frac{t-b}{a})dt \quad (1)$$

Discrete wavelet transform is calculated using equation (2).

$$DWT(a,b) = (1/\sqrt{|a|\sum_{b} x(t)\Psi_{a,b}(t)}) \quad (2)$$

$$\Psi_{a,b}(t) = \frac{1}{\sqrt{a}}\Psi(\frac{t-b}{a}) \quad (3)$$

2.3. Energy

The energy of the discrete signal x(n) in the time interval $n1 \leq n \leq n2$ is calculated by equation (4):

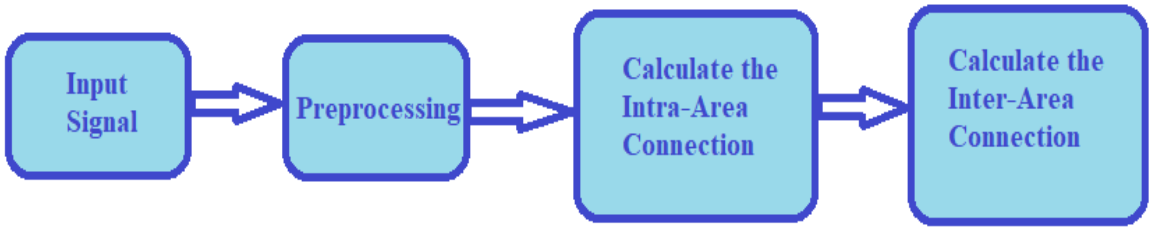

Figure 1. Flowchart of the proposed model

SCI Accepted

$$E = \sum_{n=n_1}^{n_2} |x[n]|^2 \quad (4)$$

In this article, signal energy is defined and calculated as follows [13]:

So that N is the number of di signal samples and the period is T.

$$E(I) = \sum_{i=1}^{N} d_i^2 \times T/N \quad (5)$$

2.4. Proposed Model

In this article, a model by a cellular neural network based on the structure of the brain will be presented. The model considers 17 areas, encompassing both the left and right hemisphere regions. Each area is associated with a set of electrodes. Consequently, the entire brain is represented by 17 cells, which correspond to the 17 electrodes. In this model, the input for each area is composed of the input signals received by the respective electrodes, along with feedback signals from non-adjacent areas. Furthermore, each cell within an area receives input from its corresponding electrode, as well as feedback signals from neighboring cells.

To establish the connections between the areas (electrodes), the article proposes determining the degree of connectivity. This is achieved by measuring the spectral coherence function between the electrodes, which quantifies the strength of the connections. Subsequently, the cellular neural network demonstrates the connections within each area. Both steps, determining the inter-area connections and showcasing the intra-area connections through the cellular neural network (CNN), will be explained in detail.

2.5. Spectral Coherence

In the proposed model, the coherence function is used to calculate the interaction between different channels. Coherence analysis is a non-invasive method to calculate the degree of coupling between brain channels. In this calculation, the average periodogram is used in each period with an overlap and a 50% Hamming window to reduce the effect of edges. If two channels $\xi(t)$ and $\eta(t)$ are considered with the intersection spectrum $P(f)_{\xi\square}$ and self-corresponding spectra $P(f)_{\xi\xi}$ and $P(f)_{\square\square}$, the coherence function of the two channels at each frequency is calculated by equation (6):

$$MSC(f) = \frac{|P_{\xi\eta}(f)|^2}{P_{\xi\xi}(f)P_{\eta\eta}(f)} \quad (6)$$

The value obtained from the above function is in the range of zero to one, which shows the coherence frequency of two signals related to two channels.

2.6. Cellular Neural Network

The proposed model utilizes a CNN due to its ability to capture both local and global interactions between cells, which aligns with the functioning of the brain. Since different brain areas are interconnected, the CNN is employed to calculate the connections within each area. To determine the connections between each area and other areas, the coherence function is utilized. This function quantifies the level of connectivity between different brain regions. In the proposed research, 17 channels were employed to record the brain signals, which consequently leads to the consideration of 17 areas in the model. Each area consists of a CNN network with dimensions of 4x4. Figure (2) visually depicts 16 cells within a single area. By using the CNN model and considering the connectivity and interactions between cells and areas, the proposed research aims to provide insights into the brain's functioning and the differences in connectivity patterns between individuals with hyperactivity and normal individuals.

SCI Accepted

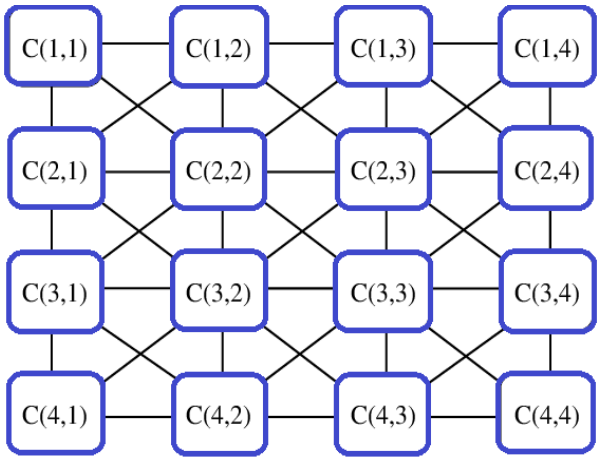

Figure 2.The structure of the cells in an area

Each of the squares in image 2 represents a cell $C(i,j)$. i shows the row of cells and j shows the column of the grid of cells. All cells and areas are connected to each other. The input is applied to each of the CNNs, then the weights and states of the cells are calculated according to the equations described below. Here, the neighborhood r=1, for $C(i,j)$ in a CNN is equal to equation (7):

$$N_r(i,j) = \{C(k,l) | \max\{|k-i|, |l-j|\} \le r, \quad 1 \le k \le M \quad (7)$$

so that r is a positive integer. The neighborhood system defined above is always displaying a set of symmetric properties for all $C(i,j)$ and $C(k,l)$ in a CNN. Each cell in the cellular neural network calculates two values: state and output, where the state value shows the state of the cell, and the output shows the degree of connection and feedback of each cell to other cells. u is the input, x is the state and y is the output of the cell. The cell state equation is as equation (8) [14].

$$\frac{dx_{ij}(t)}{dt} = -x_{ij}(t) + \sum_{(k,l)\epsilon N(i,j)} A(i,j;k,l).y_{kl}(t) + \sum_{(k,l)\epsilon N(i,j)} B(i,j;k,l).u_{kl}(t) + z(i,j;k,l) \quad (8)$$

k and l are the indices of neighboring cells. The effects of the outputs are always dependent on the interactive parameters $A(i,j;k,l)$ and the input control effect is dependent on $B(i,j;k,l)$ and z bias. The output of the cell is calculated based on equation (9) [14].

$$y_j(t) = f\left(x_{ij}(t)\right) = \left(\frac{1}{2}\right)\left(|x_{ij}(t)+1| - |x_j(t)-1|\right), \quad 1 \le i \le M; 1 \le j \le N \quad (9)$$

3. Discussion and Experimental Results

The tests were done with MATLAB software version R2022a. The proposed method has been validated using k-fold where k=10. To show the separation of the values of the two groups, SPSS statistical analysis software and t-test statistical test are used (*p*value<0.05) [13]. The simulation codes are posted in this link (https://github.com/elham09120868744/ADHD.git) for further reading.

Recordings have been obtained from 19 brain areas. Each area of the brain has direct and indirect connections and cooperation with other areas. First, to model the brain, it is necessary to obtain the degree of communication between the regions. As all areas of the brain mutually influence each other, the proposed model incorporates interconnections between each area and the others. Consequently, the correlation between the 19 channels needs to be calculated, resulting in a total of 19×18 connections. To illustrate, only a few examples of these values are provided due to the large number of columns in the table. In Table (1), the amount of connections between each two areas will be obtained.

Table 1. Mean amount of interareal connections for hyperactive and normal subjects

Electrodes	Normal mean±SD	ADHD mean±SD	(*P*value)
F7-F8	0.002±0.658	0.012±0.301	0.05

SCJ Accepted

F7-T5	0.062±0.668	0.010±0.408	0.05
F7-Pz	0.247±0.594	0.217±0.291	0.05
F7-O1	0.012±0.682	0.052±0.345	0.05
F7-O2	0.020±0.632	0.085±0.365	0.07
F8-P4	0.040±0.531	0.021±0.217	0.05
F8-T4	0.09±0.521	0.009±0.315	0.06
Cz-P3	0.008±0.478	0.020±0.781	0.05
Cz-O2	0.015±0.332	0.036±0.752	0.05
C3-O1	0.010±0.381	0.012±0.811	0.05
C3-T5	0.01±0.475	0.035±0.692	0.05
P4-P3	0.021±0.500	0.033±0.522	0.39
O1-O2	0.11±0.344	0.08±0.319	0.42

As depicted in Table (1), there are notable differences in the communication patterns between brain areas in normal individuals and those with hyperactivity (the connection values between normal individuals brain areas and ADHD are different). The results indicate that in normal individuals, there is a higher level of connectivity between the frontal areas and other regions, whereas ADHD exhibit reduced connectivity in this regard. Furthermore, it is evident that the central area of the brain in hyperactive individuals demonstrates increased connectivity with other regions compared to normal individuals, where such connections are relatively fewer. In general, the connectivity between brain areas appears to be less extensive in hyperactive individuals compared to normal individuals. The remaining connections in other normal areas were reported without significant differentiation ($p$value < 0.05). Given the disparity in connectivity patterns between brain areas in ADHDs and normal individuals, it can be inferred that the overall functioning of these two groups also differs from each other.

In the proposed model, each brain area's performance is represented by a network of CNNs. These networks consist of 19 cells, with each cell corresponding to an electrode. States and outputs (weights) of each cellular neural network are used to show the differences in intra-area connections between the brain areas of the two groups. These differences will be compared in alpha, beta and gamma bands. Table 2 displays the average weights generated by the CNN network for each brain area, along with the quantity of intra-area connections in various frequency bands. The significant differences between the two groups are denoted by +, ×, and * symbols based on t-test. The table also includes the mean (M) and standard deviation (SD) values.

Based on Table 2, noticeable differences are observed in the connectivity of cells within the frontal areas in both the alpha and beta frequency bands. Similarly, significant differences are observed in the central areas specifically in the alpha band. These findings suggest variations in the cellular connections within these regions across the two groups. Table 3 shows those states that have significant differences in each of the signal recording areas.

Table 2. The average weights of each area produced by a network of CNNs

	β Band *			**γ Band** ×			**α Band** +		
Electrodes	Normal M±SD	ADHD M±SD	*P* value	Normal M±SD	ADHD M±SD	*P* value	Normal M±SD	ADHD M±SD	*P* value
Fp1*×	0.498 ± 0.03	0.608 ± 0.121	0.00	0.594 ± 0.10	0.724 ± 0.21	0.00	0.844 ± 0.12	0.851 ± 0.13	0.21
Fp2*	0.531 ± 0.033	0.978 ± 0.02	0.00	0.589 ± 0.12	0.500 ± 0.11	0.54	0.903 ± 0.08	0.901 ± 0.05	0.45
F7*×	0.773 ± 0.03	0.530 ± 0.34	0.00	0.903 ± 0.10	0.721 ± 0.09	0.00	0.566 ± 0.05	0.525 ± 0.18	0.30

SCI Accepted

F3*×	0.925 ± 0.040	0.736 ± 0.044	0.00	0.817 ± 0.14	0.419 ± 0.22	0.00	0.752 ± 0.11	0.783 ± 0.17	0.21
F4*×	0.674 ± 0.06	0.541 ± 0.04	0.00	0.813 ± 0.09	0.701 ± 0.11	0.00	0.636 ± 0.07	0.625 ± 0.08	0.30
Fz	0.952 ± 0.04	0.852 ± 0.14	0.70	0.394 ± 0.11	0.361 ± 0.05	0.27	0.705 ± 0.32	0.799 ± 0.12	0.31
F8	0.693 ± 0.16	0.685 ± 0.26	0.41	0.681 ± 0.30	0.605 ± 0.12	0.36	0.903 ± 0.12	0.906 ± 0.13	0.21
T3	0.693 ± 0.16	0.6891 ± 0.09	0.32	0.512 ± 0.11	0.589 ± 0.22	0.24	0.337 ± 0.32	0.318 ± 0.23	0.52
C3	0.704 ± 0.16	0.301 ± 0.12	0.00	0.489 ± 0.01	0.429 ± 0.12	0.35	0.841± 0.29	0.800 ± 0.21	0.51
Cz*	0.804 ± 0.06	0.521 ± 0.08	0.00	0.911 ± 0.12	0.900 ± 0.11	0.52	0.394 ± 0.11	0.371 ± 0.09	0.15
C4*	0.895 ± 0.05	0.655 ± 0.09	0.00	0.715 ± 0.32	0.791 ± 0.11	0.38	0.748 ± 0.11	0.721 ± 0.09	0.61
T4	0.804 ± 0.21	0.794 ± 0.01	0.09	0.643 ± 0.11	0.6210 ± 0.19	0.42	0.840± 0.01	0.831 ± 0.12	0.44
T5	0.612 ± 0.21	0.691 ± 0.21	0.12	0.693 ± 0.16	0.6891 ± 0.09	0.38	0.966 ± 0.05	0.926 ± 0.15	0.32
P3*×	0.734 ± 0.15	0.444 ± 0.32	0.00	0.795 ± 0.05	0.755 ± 0.09	0.00	0.752 ± 0.12	0.751 ± 0.21	0.19
P4×	0.715 ± 0.32	0.708 ± 0.02	0.14	0.804 ± 0.06	0.521 ± 0.11	0.00	0.641 ± 0.32	0.605 ± 0.12	0.15
Pz×	0.414 ± 0.15	0.444 ± 0.32	0.00	0.695 ± 0.03	0.855 ± 0.08	0.00	0.852 ± 0.15	0.851 ± 0.11	0.19
T6	0.651 ± 0.11	0.620 ± 0.09	0.31	0.745 ± 0.32	0.702 ± 0.12	0.36	0.543 ± 0.13	0.583 ± 0.22	0.28
O1	0.907 ± 0.08	0.911 ± 0.03	0.13	0.643 ± 0.16	0.645 ± 0.28	0.52	0.337 ± 0.03	0.348 ± 0.12	0.31
O2	0.745 ± 0.11	0.721 ± 0.15	0.40	0.344 ± 0.12	0.321 ± 0.09	0.25	0.889 ± 0.01	0.829 ± 0.11	0.25

Table 3. The states that have significant differences in each of areas

Electrodes	**βBand**	**γBand**	**αBand**
Fp1	All 32 states	All 32 states	S15,1
Fp2	S1,1,S2,1,S3,1,S4,1, S5,1, S6,1, S7,1, S9,1, S10,1, S11,1, S13,1, S14,1, S15,1, S16,1, S1,2, S2,2, S3,2, S4,2, S5,2, S6,2, S7,2, S9,2, S10,2, S11,2, S13,2, S14,2, S15,2, S16,2	S7,2, S9,2	No states
F7	S1,1, S1,2, S2,2, S5,1, S6,1, S7,1, S10,1, S11,1, S15,1, S1,2, S5,2, S6,2, S7,2, S10,2, S11,2, S15,2	S2,1, S3,1, S4,1, S5,1, S6,1, S7,1, S9,1, S10,1, S11,1, S13,1, S14,1, S16,1, S1,2, S2,2, S3,2, S4,2, S5,2, S6,2, S7,2, S9,2, S10,2, S11,2, S13,2, S14,2, S15,2	S6,2
F3	S2,1, S3,1, S4,1, S5,1, S6,1, S7,1, S9,1, S10,1, S11,1, S13,1, S14,1, S16,1, S1,2, S2,2, S3,2, S4,2, S5,2, S6,2, S7,2, S9,2, S10,2, S11,2, S13,2, S14,2, S15,2	S5,1, S6,1, S7,1, S8,1, S10,1, S11,1, S12,1, S14,1, S15,1, S1,2, S6,2, S7,2, S8,2, S10,2, S11,2, S12,2, S14,2, S15,2	S11,1, S12,1
F4	S1,1,S2,1,S3,1,S4,1, S5,1, S6,1, S7,1, S9,1, S10,1, S11,1, S13,1, S14,1, S15,1, S16,1, S1,2, S2,2, S3,2, S4,2, S5,2, S6,2, S7,2, S9,2, S10,2, S11,2, S13,2, S14,2, S15,2,	S1,1, S1,2, S2,2, S5,1, S6,1, S7,1, S10,1, S11,1, S15,1, S1,2, S5,2, S6,2, S7,2, S10,2, S11,2, S15,2	No states

SCI Accepted

	S16,2		
Fz	, S3,2, S4,2, S5,2, S6,2, S7,2	S3,1,S4,1, S5,1, S6,1, S7,1	S6,1
F8	S10,2, S11,2	S15,1, S1,2, S6,2	S6,2
T3	S7,2, S9,2, S10,2	S10,2, S11,2	S7,2
C3	S5,1, S6,1, S7,1, S8,1, S10,1, S11,1, S12,1, S14,1, S15,1, S1,2, S6,2, S7,2, S8,2, S10,2, S11,2, S12,2, S14,2, S15,2	S8,1, S10,1	, S6,2
Cz	S2,1, S3,1, S4,1, S5,1, S6,1, S7,1, S9,1, S10,1, S11,1, S13,1, S14,1, S16,1, S1,2, S2,2, S3,2, S4,2, S5,2, S6,2, S7,2, S9,2, S10,2	S11,1, S2,2	No states
C4	All States	S12,1, S13,1, S1,2	S8,2
T4	S5,2, S8,2	S11,1, S13,1	No states
T5	S9,2, S10,2, S11,2	No states	S7,1, S9,1
P3	1,1, S2,1, S6,1, S7,1, S8,1, S9,1, S11,1, S12,1, S13,1, S1,2, S2,2, S6,2, S7,2, S8,2, S9,2, S11,2, S12,2, S13,2	S3,1, S4,1, S5,1, S8,1, S9,1, S10,1, S11,1, S2,2, S3,2, S4,2, S5,2, S8,2, S9,2, S10,2, S11,2, S13,2, S14,2, S16,2	S5,2, S8,2
P4	S11,1, S13,1	S2,1, S3,1, S4,1, S5,1, S6,1, S7,1, S9,1, S10,1, S11,1, S13,1, S14,1, S16,1, S1,2, S2,2, S3,2, S4,2, S5,2, S6,2, S7,2, S9,2, S10,2, S11,2, S13,2, S14,2, S15,2	S2,2, S3,2, S4,2, S5,2
Pz	S1,2, S2,2	S1,1,S2,1,S3,1,S4,1, S5,1, S6,1, S7,1, S9,1, S10,1, S11,1, S13,1, S14,1, S15,1, S16,1, S1,2, S2,2, S3,2, S4,2, S5,2, S6,2, S7,2, S9,2, S10,2, S11,2, S13,2, S14,2, S15,2, S16,2	S9,1
T6	S11,1, S12,1	S7,2, S8,2	No states
O1	S7,2, S10,2, S11,2	S14,2, S15,2	No states
O2	S8,2, S10,2	S7,2, S8,2, S10,2	S11,2

The alpha band typically manifests when the eyes are closed and the brain is in a relaxed state. The individuals involved in this research were engaged in character recognition and identification tasks during the signal recording, therefore, the alpha band does not appear prominently in the results of these individuals. Moreover, Table 2 and 3 demonstrate no noticeable variations across different areas in the alpha band. On the other hand, the gamma band intensifies during alertness and cognitive processing. Based on the alertness levels of the subjects under examination, significant differences (P value < 0.05) can be observed in the Fp1, F7, F3, and Fp2 channels. Additionally, significant differences were observed in the central areas, specifically the C3, Cz, and C4 channels. In the P3 electrode, distinct differences were also visible in the terminal part. However, no differences were observed in the T and occipital areas. The beta band is associated with wakefulness and active mental states. Accordingly, evident differences can be observed in the Fp1, F7, F3, P4, and P3 channels, as indicated in Table 2 and 3.

Based on the experimental results, it can be concluded that hyperactive individuals exhibit not only differences in inter-areal communication, encompassing the central, frontal, and parietal areas, but also noticeable differences in intra-areal communication involving the electrodes within these areas.

To compare the accuracy of the values obtained from the proposed model and validate its effectiveness, the values were evaluated using Convolutional Neural Network [24], Recurrent Neural Network (RNN), and SVM [25] methods.

SCI Accepted

The CNN used in the proposed method is a 3D, with 6 hidden layers. It applies a convolutional layer with a 4x2x20 filter bank to the input, and in the pooling layer, the filter bank size is 2x2x20, resulting in an output size of 319x7x20. The values obtained from these methods, specifically focusing on the β band, were used to separate the two groups: ADHD and normal. The performance of each method is presented in Table 4. To mitigate the risk of overfitting, the methods were trained and evaluated using 10-fold cross-validation.

Table 4. Evaluation of the performance of three methods based on the obtained values from proposed model

Criteria	Convolutional Neural Network	RNN	SVM
Accuracy	95.85	92.8	81.2
Precision	93.8	91.9	86.9
Recall	94.9	93.05	83.4

Indeed, the results indicate that the values obtained from the proposed model are accurate and capable of effectively separating the two groups. Table 4 clearly demonstrates that the Convolutional Neural Network (CNN) method achieves higher accuracy in classification compared to the other methods. This suggests that the CNN model is more reliable and proficient in accurately categorizing the individuals into their respective groups.

4. Conclusion

Hyperactivity disorder is a behavioral disorder characterized by an individual's inability to pay attention and maintain focus on a subject. Research has provided evidence of differences in brain structure and electroencephalographic (EEG) signals among individuals with hyperactivity disorder. In this article, an intelligent and efficient model was employed to identify distinct areas associated with hyperactivity.

The models that have been presented so far, based on the brain connections of individuals with ADHD, have been primarily statistical in nature. However, this article introduces an innovative approach by employing an intelligent model to analyze the brain connections of both ADHD and normal individuals. Unlike previous studies that focused solely on EEG and its features, this article takes into account the brain connections of both groups. The results demonstrate significant differences in brain connections between the two groups. Leveraging a convolutional neural network, the proposed model achieved high accuracy in distinguishing between individuals with ADHD and those without.

The proposed model estimated the intra-areal connections of the brain in hyperactive individuals by utilizing the spectral coherence function between different channels. Subsequently, the intra-areal connections were obtained using a CNN operating in the beta, alpha, and gamma frequency bands. Based on the obtained results, it can be concluded that individuals with hyperactivity disorder exhibit not only differences in inter-areal communication, encompassing the central, frontal, and parietal areas, but also significant differences in intra-areal communication within these areas, particularly in the beta and gamma frequency bands during states of processing and alertness.

The results confirmed the validity of the values obtained from the proposed model. Moreover, these values demonstrated a high accuracy in effectively separating the ADHD and normal groups. This suggests that the proposed model and the derived values have significant potential as a reliable tool for accurately distinguishing between individuals with ADHD and those without it.

5. Conflict of Interest

The authors confirm that they have no affiliation or involvement in any organization or entity with any financial interest such as fees, fellowships, speaker's bureau participation; Membership, employment, consulting, stock ownership, or other stock interests; and expert certificate or patent license arrangements or non-financial interests such as personal or professional relationships, affiliations, knowledge or

SCJ Accepted

beliefs in the topic or content discussed in this article.

Acknowledgements

This study has been adapted from a research project at Islamic Azad University, Fouman and Shaft Branch.

Funding

The study was funded by the research part of Fouman and Shaft Branch for Islamic Azad University, Fouman and Shaft Branch. (No.40139926).

References

[1]Boonstra A., Kooij J., Osterlaan J., Sergent J. A., Buitelaar K. J., "Dose methylphenidate improve inhibition and other cognitive abilities in adults with childhood onest ADHD?" *Journal of Clinical and Exceptional Neurobiology*. Vol. 27, pp. 278-298, 2005. doi: 10.1080/13803390490515757.

[2] Brock S. E., Jemerson S. R., Hansen R. L., Developmental psychopathological at school: Identifying, assessing and treating ADHD at school, Springer. 2009.

[3] Müller A A., Vetsch S., IPershin I., Candrian G., Baschera G. D., Kropotov J., Kasper J., "EEG/ERP-based biomarker/neuroalgorithms in adults with ADHD: Development, reliability, and application in clinical practice". *The World Journal of Biological Psychiatry*. pp.1-12. 2019. DOI: 10.1080/15622975.2019.1605198

[4] Baijot S., Slama H., Söderlund G., Dan B., Deltenre P., Colin C., Deconinck N., "Neuropsychological and neurophysiological benefits from white noise in children with and without ADHD". *Behav. Brain Funct*. Vol. 12, 2017. 10.1186/s12993-016-0095-y

[5] Askari E., Setarehdan S.K., Sheikhani A., Mohamadi M.R., Teshnelab M., "Designing a model to detect the brain connections abnormalities in children with autism using 3D-cellular neural networks". J*ournal of Integrative Neuroscience*. Vol. 17(3-4). pp.391-411, 2018. DOI: 10.3233/JIN-180075.

[6] Mueller A., Candrian G., Kropotov J.D, Ponomarev V.A., Baschera G.M., "Classification of ADHD patients on the basis of independent ERP components using a machine learning system". *Nonlinear Biomedical Physics*. Vol. 4, 2010. doi: 10.1186/1753-4631-4-S1-S1

[7] Mueller A., Candrian G., Arntsberg Grane V., Kropotov J.D., Ponomarev V.A., Baschera G.M., "Discriminating between ADHD adults and controls using independent ERP components and a support vector machine: a validation study". *Nonlinear Biomedical Physics*. Vol. 5(1), 2011. doi: 10.1186/1753-4631-5-5.

[8] Chandana S., Balaraj K., Sushmitha P., Usha P., "Extraction and Analysis of EEG signals for the detection of ADHD syndrome – A novel approach". *A project Report*. 2016. doi.org/10.1016/j.heliyon.2024.e26028.

[9] Moriguchi Y., Hiraki K.. "Neural origin of cognitive shifting in young children". *In Proceedings of the National Academy of Sciences of the United States of America*. Vol. 106. pp.6017-6021, 2009. doi.org/10.1073/pnas.0809747106.

[10] Negoro H., Sawada M., Iida J., Ota T., Tanaka S., Kishimoto T., "Prefrontal dysfunction in attention-deficit/hyperactivity disorder as measured by near-infrared spectroscopy". *Child Psychiatry & Human Development*. Vol. 41. pp. 193-203, 2010. doi: 10.1007/s10578-009-0160-y

[11] Cortes C., Vapnik V., "Support-vector networks". *Machine Learning*. Vol. 20. pp. 273-297, 1995. doi.org/10.1007/BF00994018.

SCJ Accepted

[12] Akira Yasumura A., Omori M., Fukuda Y., Takahashi J., "Applied Machine Learning Method to Predict Children With ADHD Using Prefrontal Cortex Activity: A Multicenter Study in Japan". *Journal of Attention Disorders.* 24(14), 2017. doi.org/10.1177/1087054717740.

[13] Metsis V., Makedon F., Shen D., Huang H., V Metsis., F Makedon., D Shen., H Huang., "DNA Copy Number Selection Using Robust Structured Sparsity-Inducing Norms". *IEEE/ACM Transactions on Computational Biology and Bioinformatics.* Vol. 11(1). Pp., 2014.168-181. doi: 10.1109/TCBB.2013.141.

[14] Askari E., Setarehdan S K., Sheikhani A., Mohamadi M R., Teshnelab M., "Modeling the connections of brain areas in children with autism using cellular neural networks and electroencephalography analysis". *Artificial Intelligence in Medicine*. Vol. 89: 40-50, 2018. doi.org/10.1016/j.artmed.2018.05.003.

[15] Mohammadi M R., Khaleghi A., Moti Nasrabadi A., Rafieivand S., Begol M., "EEG Classification of ADHD and Normal Children Using Non-linear Features and neural network". *Biomedical Engineering Letters springer*. 2016. doi: 10.1007/s13534-016-0218-2.

[16] Moqadam R., Loghmani N., Moghaddam A., Allahverdy A., "Differentiating Brain Connectivity Networks in ADHD and Normal Children using EEG". *in 30th International Conference on Electrical Engineering (ICEE)*. 2022. doi: 10.1109/ICEE55646.2022.9827093

[17] He Y., et al., "Brain Network Connectivity Analysis of Different ADHD Groups Based on CNN-LSTM Classification Model". in *International Conference on Intelligent Robotics and Applications(ICIRA)*. pp. 626–635. 2022.

[18] Motamed S., Askari E., "Recognition of Attention Deficit/Hyperactivity Disorder (ADHD) Based on Electroencephalographic Signals Using Convolutional Neural Networks (CNNs)". *Journal of Information Systems and Telecommunication (JIST)*. Vol. 10, 2022. doi:rimag.ricest.ac.ir/fa/Article/16399/FullText.

[19] TaghiBeyglou B., Shahbazi A., Bagheri F., Akbarian S., Jahed M., "Detection of ADHD cases using CNN and classical classifiers of raw EEG". *Computer Methods and Programs in Biomedicine Update*. Vol. 2, 2022. doi: /10.1016/j.cmpbup.2022.100080.

[20] Wen Loh H., et al. "Deep neural network technique for automated detection of ADHD and CD using ECG signal". *Computer Methods and Programs in Biomedicine*. Vol. 241, 2023. doi.org/10.1016/j.cmpb.2023.107775.

[21] Bakhtiyari M., Mirzaei S., "ADHD Detection UsingDynamic Connectivity Patterns of EEG Data and ConvLSTM with Attention Framework". *Biomedical Signal Processing and Control.* Vol. 76, 2022. doi.org/10.1016/j.bspc.2022.103708.

[22] Holker H., Susan S., "Computer-Aided Diagnosis Framework for ADHD Detection Using Quantitative EEG". in *International Conference on Brain Informatics*. pp. 229–240, 2022.

[23] Sharifi Mehrjard, Z., Momeni, H., Adabi Ardekani, H. A review of machine learning algorithms to diagnose autism using EEG signal. *Soft Computing Journal*, 2023; doi: 10.22052/scj.2023.248522.1110. [In Persian]

[24]Eftekharian M., Nodehi A., "Breast Cancer Diagnosis and Classification Improvement based on Deep Learning and image Processing methods". *Soft Computing Journal*, 2022; doi: 10.22052/scj.2023.246416.1067.

[25] Mirzakhani, A., Mohammadpoor, M. Detection of Disc Destruction Between Lumbar Vertebrae Using MRI Images. *Soft Computing Journal*, 2021; 9(1): 114-123. doi: 10.22052/scj.2021.111454. [In Persian]

SCJ Accepted